Influence of reducing anneal on the ferromagnetism in single crystalline Co-doped ZnO thin films*

Lu Zhong-Lin(路忠林)[a)b)†], Zou Wen-Qin(邹文琴)[c)],
Xu Ming-Xiang (徐明祥)[a)], and Zhang Feng-Ming(张凤鸣)[c)]

[a)] *Department of Physics, Southeast University, Nanjing* 210096, *China*
[b)] *Physics Department and Institute of Innovations and Advanced Studies (IIAS), National Cheng Kung University, Tainan* 701, *China*
[c)] *Jiangsu Provincial Laboratory for Nanotechnology, National Laboratory of Solid State Microstructure, and Department of Physics, Nanjing University, Nanjing* 210093, *China*

(Received 29 August 2009; revised manuscript received 23 September 2009)

This paper reports that the high-quality Co-doped ZnO single crystalline films have been grown on a-plane sapphire substrates by using molecular-beam epitaxy. The as-grown films show high resistivity and non-ferromagnetism at room temperature, while they become more conductive and ferromagnetic after annealing in the reducing atmosphere either in the presence or absence of Zn vapour. The x-ray absorption studies indicate that all Co ions in these samples actually substituted into the ZnO lattice without formatting any detectable secondary phase. Compared with weak ferromagnetism (0.16 $\mu_{\rm B}/{\rm Co}^{2+}$) in the $Zn_{0.95}Co_{0.05}O$ single crystalline film with reducing annealing in the absence of Zn vapour, the films annealed in the reducing atmosphere with Zn vapour are found to have much stronger ferromagnetism (0.65 $\mu_{\rm B}/{\rm Co}^{2+}$) at room temperature. This experimental studies clearly indicate that Zn interstitials are more effective than oxygen vacancies to activate the high-temperature ferromagnetism in Co-doped ZnO films, and the corresponding ferromagnetic mechanism is discussed.

Keywords: Co-doped ZnO, diluted magnetic semiconductors, x-ray absorption fine structure, single crystalline thin films

PACC: 6110M, 7550P, 7280E, 7870D

1. Introduction

The ZnO semiconductor has gained substantial interest in the research community for its wide prospects in optoelectronic applications, such as ultraviolet light emitters, sensors, displays, solar cells, etc., owing to its direct wide band gap of ∼3.37 eV and large excitonic binding energy of 60 meV at room temperature (RT).[1−4] Currently, ZnO-based diluted magnetic semiconductors (DMSs), which involve the charge and spin degrees of freedom of electrons in a single substance, are attracting much more attention due to their potential applications in 'spintronics' devices.[5,6] Theoretically, Dietl *et al.* first predicted that p-type Mn doped ZnO would show ferromagnetism with $T_{\rm C}$ well above RT.[7] However, ZnO is intrinsically n-type conducting and the p-type ZnO with high hole concentration is notoriously difficult to realize experimentally.[8] In contrast to Mn doped ZnO, Co doped ZnO was theoretically predicated to become ferromagnetic with n-type doping[9] and a flood of experimental studies of this subject have been reported upon.[10−20] However, the presented data were plagued by instability and a lack of reproducibility. In some cases, the ferromagnetism can be attributed to uncontrolled ferromagnetic clusters or secondary phases,[10,11] which is absent from single phase specimens.[12] However, in many other cases, high-temperature ferromagnetism could have been caused by defects, including Zn interstitials (Zn_i) and oxygen vacancies (V_O) which are presented in the TM-doped ZnO, as explained by the bound magnetic polaron (BMP) model.[13,14] Schwartz and Gamelin[15] firstly reported a reversible ferromagnetic ordering in Co-doped ZnO nanocrystals and films by lattice incorporation and removal of the native n-type defects,

*Project partially supported by National Science Foundation of China (Grant No. 10804017), National Science Foundation of Jiangsu Province of China (Grant No. BK2007118), Research Fund for the Doctoral Program of Higher Education of China (Grant No. 20070286037), Cyanine-Project Foundation of Jiangsu Province of China (Grant No. 1107020060), Foundation for Climax Talents Plan in Six-Big Fields of Jiangsu Province of China (Grant No. 1107020070) and New Century Excellent Talents in University (NCET-05-0452).
†Corresponding author. E-mail: linzi077@163.com
© 2010 Chinese Physical Society and IOP Publishing Ltd

Zn_i. While Hsu *et al.*[16] demonstrated that the ferromagnetism in Co-doped ZnO DMSs should be strongly correlated with V_O in ZnO. In fact, the defect chemistry of ZnO is very complex, with Zn interstitials, Zn vacancies, oxygen interstitials and vacancies all known to be presented in varying concentrations.[21] Usually, the predominant defects in ZnO are Zn_i and/or V_O, which depend on the growth and post-annealing conditions. In the present work, we used molecular beam epitaxy (MBE) to grow high-quality Co-doped ZnO single crystalline films with very low residual carrier concentration. Compared with neglectable ferromagnetism in the as-deposited films, the films became good conductive and ferromagnetic after annealing in the reducing atmosphere both in the presence and absence of Zn vapour. After careful and systematic studies on the structural and magnetic properties, we clearly demonstrate that Zn interstitials are more effective than oxygen vacancies to induce high-temperature ferromagnetism in Co-doped ZnO films.

2. Experiment

Co-doped ZnO ($Zn_{0.95}Co_{0.05}O$) thin films with a thickness of 500 Å were prepared in an MBE system with a base pressure of 5×10^{-8} Pa on Al_2O_3 $(11\bar{2}0)$ substrate at 400 °C using the δ-doping technique.[22] A 50 Å pure ZnO film was grown on the substrate as a buffer layer before the Co-doped film was deposited. Pure (99.995%) ZnO and Co in a ratio of 20 : 1 were evapourated from two independent e-beam sources. The oxygen pressure was kept to be 1×10^{-4} Pa to control the oxygen stoichiometry and the typical deposition rate was about 0.02 Å/s (1 Å= 0.1 nm). Sequential post-annealing of the as-deposited $Zn_{0.95}Co_{0.05}O$ thin films were performed by sealing the films in an evacuated quartz tube in the presence or absence of metallic Zn. The samples were then annealed at 500 °C for 60 min, and then cooled to RT. Oxidative annealing was undertaken in the same system at 500 °C for 60 min in flowing oxygen atmosphere. The atomic concentrations of the doping element were checked by energy dispersive x-ray analysis (EDAX). The film structure and crystalline quality were determined by *in situ* high-energy electron diffraction (RHEED) and high-resolution x-ray diffraction (XRD) at the BL17B beamline of the Taiwan Light Source (TLS) in Hsinchu, Taiwan. The x-ray-absorption fine structure (XAFS) measurements of the Zn and Co K-edges were performed in the wiggler-C beamline of TLS to determine the electronic state and local environment of the Zn and Co in the doped films. Magnetization studies were carried out by using a superconducting quantum interference device (SQUID) magnetometer (MPMS, XL-7T) in the temperature range 5–350 K. Electrical transport including Hall measurements was carried out by using a four terminal van der Pauw configuration in magnetic fields up to 1 T.

3. Results and discussion

Because of neglectable lattice mismatch (< 0.1%) between ZnO(0001) and $Al_2O_3(11\bar{2}0)$,[23] epitaxial growth of high-quality $Zn_{0.95}Co_{0.05}O$ films were realized on a-plane sapphire substrates. For the as-deposited films, clear c-oriented ZnO $[10\bar{1}0]$ and $[11\bar{2}0]$ streaky *in situ* RHEED patterns were observed (Fig. 1(a) inset), indicating the doped ZnO epilayers were grown in the two-dimensional layer-by-layer growth model.[24] The out-of-plane and in-plane orientational relationships are ZnCoO [0001]//sapphire $[11\bar{2}0]$ and ZnCoO $[11\bar{2}0]$//sapphire [0001]. It seems that the as-grown $Zn_{0.95}Co_{0.05}O$ samples are high-quality single crystalline thin films with atomic flat surface morphology, which are suitable for multilayer devices. High-resolution XRD measurements of both the as-grown and post-annealed films were performed and shown in Fig. 1(a). Clearly, all of the doped films exhibit a strong c-axis texture without any detectable second phase, suggesting that the doped Co ions could be as substitution into ZnO lattice. The full width at half maximum (FWHM) of (0002) peak is below 0.20°, indicating excellent crystallinity of the doped films. The typical ϕ scan from a $(10\bar{1}1)$ plane of the as-grown $Zn_{0.95}Co_{0.05}O$ sample was also performed to verify its single crystalline characteristics, as shown in Fig. 1(b). The sixfold symmetry of the ZnO hexagonal structure crystal basal plane is clearly revealed by the six peaks separated by 60°. The FWHM of the peaks is about 1.4°, revealing very good epitaxy.

As is well known, even there is no evidence of any secondary phases by XRD measurements, the secondary phases, such as metallic Co, in trace amounts and small clusters which below the detection limit of XRD are still possibly hidden in the Co-doped ZnO thin films.[25] On the contrary, XAFS based on synchronization radiation has been considered to be one

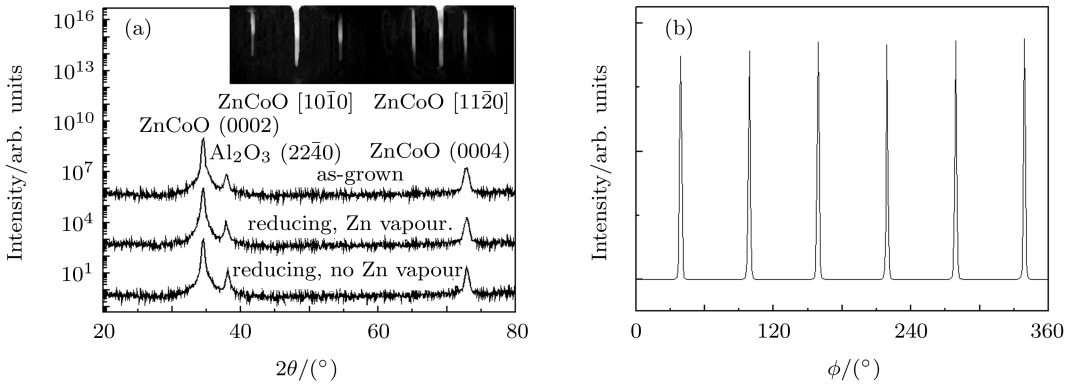


Fig. 1. (a) x-ray θ–2θ scans of the as-grown $Zn_{0.95}Co_{0.05}O$ thin film, and films annealed at 500 °C for 60 min in a reducing atmosphere with and without Zn vapour, respectively. (b) A typical ϕ-scan from a (10$\bar{1}$1) plane of the as-grown $Zn_{0.95}Co_{0.05}O$ thin film. The inset shows its corresponding RHEED patterns.

of the most useful and powerful techniques in this area and is very sensitive to formation of metal bonding to the level of a few percent of the dopant atoms.[26] Here the electronic state and local environment of the doped Co ions in all the films were studied by XAFS. The x-ray absorption near-edge structure (XANES) is highly sensitive to the electronic structure of doped ions in host oxides. Figure 2(a) shows the Co K-edge XANES spectra of the as-deposited and post-annealed $Zn_{0.95}Co_{0.05}O$ thin films as well as those of the standard Co metal and the oxides for comparison. In contrast to the marked shoulder around 7712 eV for the Co metal, the Co K-edge spectra of all the samples show clear 1s to 3d pre-edge features around 7709 eV, which are characteristic of Co^{2+} substitution for Zn^{2+} in ZnO.[27] Additionally, it is clear that for all samples, the Co absorption edge rises at the same photon energy as CoO, indicating that Co ions in all the samples might be in the divalent Co^{2+} valence states. The sensitivity of XANES to Co^0 is limited to below 5% of the Co dopants forming metallic Co; smaller fractions of Co^0 would be difficult or impossible to detect. Extended XAFS (EXAFS) is also adopted to clarify the local structures around the Co atoms. Figure 2(b) plots the radial distribution function (RDF), the Fourier transform amplitude of EXAFS, at the Co and Zn K-edge for all the samples. For the Zn RDF, the first and second peaks observed can be identified as Zn–O and Zn–Zn bonding, respectively. The RDFs for all the films at the Co K-edge are very similar to those of the Zn K-edge spectra, implying that Co ions have similar local structures, as do the Zn ions in ZnO. The EXAFS results reveal that nearly all Co atoms actually substitute into the ZnO lattice without the formation of any detectable metallic Co or other secondary phase. In summary, XAFS studies provide strong evidence that there is no change in the Co^{2+} speciation and no phase segregation upon reducing annealing either in the presence or absence of metallic Zn vapour.

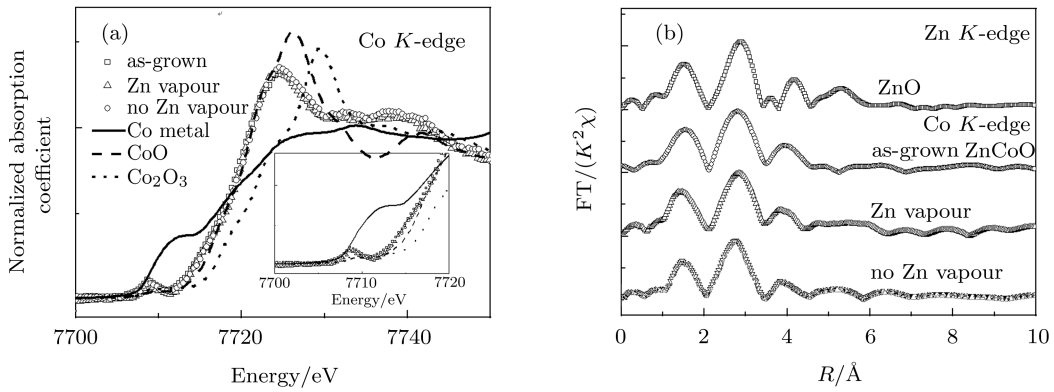


Fig. 2. (a) Normalized absorption spectra of the as-grown $Zn_{0.95}Co_{0.05}O$ thin film, and films annealing treatment with and without Zn vapour on Co K-edges, and (b) the radial distribution functions of Co from Fourier transform magnitude of EXAFS of Co K-edges, respectively.

Measurements of the resistivity and Hall effect of the as-grown and post-annealed $Zn_{0.95}Co_{0.05}O$ thin films were made, and the data are shown in Table 1. The as-grown $Zn_{0.95}Co_{0.05}O$ thin films are highly resistive ($> 50\Omega\cdot$cm), which is indicative of near oxygen-stoichiometric films with low structural defects. Upon the reducing annealing with and without Zn vapour, the resistivity ρ of the $Zn_{0.95}Co_{0.05}O$ film greatly decreases several orders of magnitude, down to 4.6×10^{-2} and $5.4\times10^{-2}\Omega\cdot$cm, respectively, because of the presence of a large carrier concentration n_c. The large carrier concentration is introduced by the high-density V_O and/or Zn_i defects, which are the shallow donors in ZnO semiconductor and easily generated upon annealing in the reducing atmosphere. Usually, the predominant defects are V_Os upon annealing in vacuum, while a lot of additional Zn_i defects would be introduced by annealing in the presence of Zn vapour.[28] Here we noted that carrier concentration of the film annealed in the reducing atmosphere with Zn vapour (1.1×10^{19} cm^{-3}) was higher than that without Zn vapour (1.0×10^{19} cm^{-3}), revealing that the presence of additional Zn_i defects induced by the Zn vapour increased the carrier concentration, as expected. On the other hand, the difference of carrier concentration is only 10%, indicating that the number of induced carriers by Zn_i defects through Zn vapour is much smaller in comparison with the concentration of V_Os, which is well consistent with the results reported by other groups.[29]

Table 1. Electrical and magnetic parameters at 300 K of the as-deposited and post-annealed $Zn_{0.95}Co_{0.05}O$ thin films. (1 Oe = 79.5775 A/m)

sample	$\rho/(\Omega\cdot\text{cm})$	n_c/cm^{-3}	$\mu/(\text{cm}^2\cdot\text{V}^{-1}\cdot\text{s}^{-1})$	$M_S/(\mu_B/\text{Co}^{2+})$	H_C/Oe
as-grown	> 50	-	-	0	0
Zn vapour	4.6×10^{-2}	1.1×10^{19}	12.4	0.65	110
no Zn vapour	5.4×10^{-2}	1.0×10^{19}	11.6	0.16	80

The field dependence of in-plane magnetization of the as-deposited and post-annealed $Zn_{0.95}Co_{0.05}O$ thin films was measured at 300 K, as shown in Fig. 3(a). To eliminate the influence of substrates, the M–H curves of the films were obtained after the contribution of the sapphire substrate had been subtracted. The as-deposited $Zn_{0.95}Co_{0.05}O$ thin film has nearly no ferromagnetic signal at 300 K, indicating all of the doped Co ions are in paramagnetic and/or antiferromagnetic coupling due to few structural defects in the high-quality single crystalline films, as expected. On the contrary, upon annealing in the reducing atmosphere, the doped films show clear ferromagnetic hysteresis loops at 300 K, suggesting that the ferromagnetic ordering of doped Co ions is effective to be activated by the reducing annealing. It is also noticed that the ferromagnetism in the post-annealed film without Zn vapour is very weak with a low magnetic moment (M_s) of only 0.16 μ_B/Co^{2+} and coercive field (H_c) of 80 Oe at 300 K. Comparatively, the ferromagnetism became much stronger after reducing annealing in the presence of Zn vapour, and the corresponding M_s and H_c reach 0.65 μ_B/Co^{2+} and 110 Oe at 300 K, respectively. As discussed above, the free carrier concentration is almost similar in the post-annealed $Zn_{0.95}Co_{0.05}O$ films with or without Zn vapour, suggesting that the free carrier concentration is not the key factor in determining the ferromagnetism. In other words, the significantly enhanced ferromagnetism is reasonable to be attributed to the high-density Zn_i defects introduced by Zn vapour, which have been considered to play an important role in mediating the ferromagnetism in Co-doped ZnO thin films.[28,29] The ferromagnetic mechanism can be understood in the framework of the BMP model in which ferromagnetic exchange is mediated through localized donor electrons in the Zn_i impurity band.[30] Exchange interactions between one localized carrier introduced by Zn_i and many surrounding Co^{2+} ions aligned all the Co^{2+} spins around the carrier localization centre, forming a BMP. The overlapping of neighbouring BMPs can result in the long range Co^{2+}–Co^{2+} ferromagnetic coupling in the $Zn_{0.95}Co_{0.05}O$ thin films. Moreover, in order to shed light on the magnetic origin in the post-annealed $Zn_{0.95}Co_{0.05}O$ films, both the zero-field-cooled (ZFC) and field-cooled (FC) magnetizations as a function of temperature at applied field of

50 Oe were measured, and the results for the post-annealed films with and without Zn vapour are shown in Fig. 3(b). Clearly, the ZFC curves appear rather smooth between 300 K and 20 K and no blocking temperature due to ferromagnetic nano-clusters could be seen. Furthermore, it is found that the FC $M(T)$ data can be well fitted by a standard block spin-wave model ($M(T) = M_0(1-AT^{3/2})$,[31] where M_0 is the zero temperature magnetization, added a Curie–Weiss model ($\chi = \chi_0 + C/(T-\theta)$), revealing a mixed magnetic phase, i.e. a ferromagnetic phase plus a paramagnetic one. Indeed, there is just a fraction of doped Co^{2+} ions in ferromagnetic ordering and the others are still in paramagnetic or antiferromagnetic ordering, with consideration that the saturated magnetic moment is only several tenths μ_B/Co^{2+}, much below the expected value of 3 μ_B/Co^{2+} for tetrahedrally coordinated high-spin Co^{2+} ions.

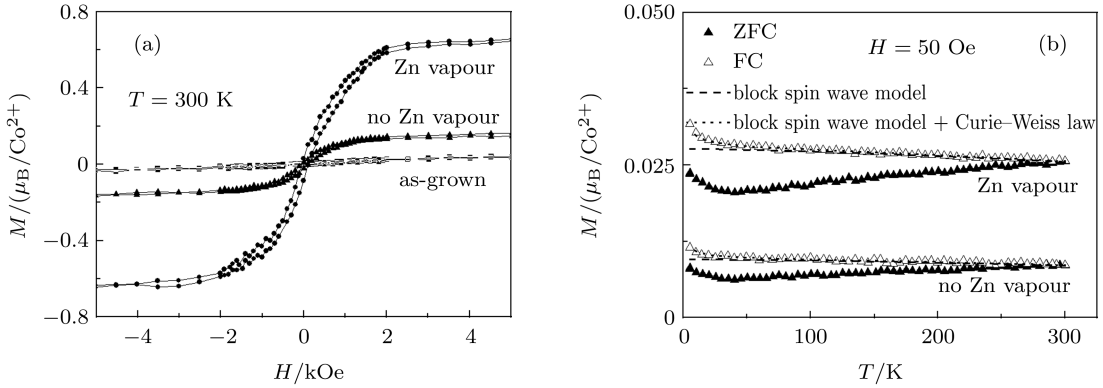


Fig. 3. (a) Magnetic hysteresis loops measured at 300 K with the applied magnetic field parallel to the film plane for the as-grown and post-annealed $Zn_{0.95}Co_{0.05}O$ thin films. (b) Magnetization of the post-annealed $Zn_{0.95}Co_{0.05}O$ thin films as a function of temperature in a field of 50 Oe with ZFC and FC. The fitting results of the FC data are also shown.

Finally, the reversibility of the RT ferromagnetism in $Zn_{0.95}Co_{0.05}O$ single crystalline thin films was studied by alternately reducing and oxidizing annealing of the films, as shown in Fig. 4. The results of the first reducing annealing of the as-deposited films have been discussed in detail above. Oxidizing the post-annealed thin films was performed by heating them at 500 °C for 60 min in flowing oxygen atmosphere. Interestingly, all of the films became insulating and non-ferromagnetic after oxidization, i.e. returned to their original as-deposited state. Furthermore, re-reducing annealing of the same films with or without Zn vapour also can returned them quantitatively to the conductive and ferromagnetic state which they had after the first reduction. The chemical perturbation that leads to RT ferromagnetism in $Zn_{0.95}Co_{0.05}O$ single crystalline thin films is therefore fully and quantitatively reversible. It indicates that the switching of the magnetic state is most likely to arise from incorporation or removal of Zn_i and/or V_O into the lattice of non-ferromagnetic high-quality $Zn_{0.95}Co_{0.05}O$, which activates ferromagnetism by forming a large number of BMPs. Considering that much stronger ferromagnetism can be activated by reducing annealing with additional Zn vapour, we know that Zn_i defects are more effective than V_O defects to mediate high-temperature ferromagnetism in Co-doped ZnO films.

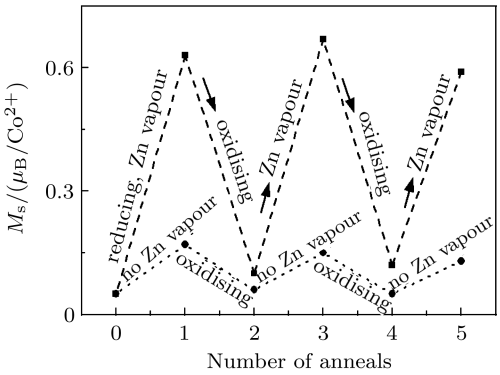


Fig. 4. Variation of the saturation moment at 300 K of the $Zn_{0.95}Co_{0.05}O$ thin film alternately annealed in a reducing atmosphere with and without Zn vapour, and an oxidizing atmosphere.

4. Conclusions

In summary, high-quality $Zn_{0.95}Co_{0.05}O$ single crystalline films have been grown on a-plane sapphire by MBE. The as-deposited films showed high resistivity and neglectable ferromagnetism at RT, and annealing in the reducing atmosphere induces ferromagnetism and low resistivity. Compared with weak ferromagnetism (0.16 μ_B/Co^{2+}) in the $Zn_{0.95}Co_{0.05}O$ thin film after reducing annealing in the absence of Zn vapour, the film annealed in the reducing atmosphere with Zn vapour is found to have much stronger ferromagnetism (0.65 μ_B/Co^{2+}) at RT. Our experimental observations clearly indicate that Zn interstitials are more effective than oxygen vacancies to activate the high-temperature ferromagnetism in Co-doped ZnO films by forming a large number of BMPs.

References

[1] Cho S, Ma J, Kim Y, Sun Y, Wong G K L and Ketterson J B 1999 *Appl. Phys. Lett.* **75** 2761

[2] Cao H, Xu J Y, Seeling E W and Chang R P H 2000 *Phys. Rev. Lett.* **84** 5584

[3] Tsukazaki A, Ohotmo A, Onuma T, Ohtani M, Makino T, Sumiya M, Ohtani K, Chichibu Shigefusa F, Fuke S, Segawa Y, Ohno H, Koinuma H and Kawasaki M 2005 *Nat. Mater.* **4** 42

[4] Xu H Y, Liu Y C, Mu R, Shao C L, Lu Y M, Shen D Z and Fan X W 2005 *Appl. Phys. Lett.* **86** 123107

[5] ÖzgürÜ, Alivov Ya I, Liu C, Teke A, Reshchikov M A, Doğan S, Avrutin V, Cho S J and Morkoc H 2005 *J. Appl. Phys.* **98** 041301

[6] Janisch R, Gopal P and Spaldin N A 2005 *J. Phys. Condens. Matter.* **17** R657

[7] Dietl T, Ohno H, Matsukura F, Cubert J and Ferrand D 2000 *Science* **287** 1019

[8] Wang Q, Sun Q, Jena P and Kawazoe Y 2004 *Phys. Rev.* B **70** 052408

[9] Sato K and Katyama-Yoshida H 2002 *Semicon. Sci. Technol.* **17** 367

[10] Peng X D, Zhu T and Wang F W 2009 *Acta Phys. Sin.* **58** 3274 (in Chinese)

[11] Yan G Q, Xie K X, Mo Z R, Lu Z L, Zou W Q, Wang S, Yue F J, Wu D, Zhang F M and Du Y W 2009 *Acta Phys. Sin.* **58** 1237 (in Chinese)

[12] Sati P, Deparis C, Morhain C, Schäfer S and Stepanov A 2007 *Phys. Rev. Lett.* **98** 137204

[13] Coey J M D, Venkatesan M and Fitzgerald C B 2005 *Nat. Mater.* **4** 173

[14] Liu X C, Shi E W, Chen Z Z, Zhang H W, Zhang T and Song L X 2007 *Chin. Phys.* **16** 1770

[15] Schwartz Dana A and Gamelin Daniel R 2004 *Adv. Mater.* **16** 2115

[16] Hsu H S, Huang J C A, Huang Y H, Liao Y F, Lin M Z, Lee C H, Lee J F, Chen S F, Lai L Y and Liu C P 2006 *Appl. Phys. Lett.* **88** 242507

[17] Cheng X W, Li X, Gao Y L, Yu Z, Long X and Liu Y 2009 *Acta Phys. Sin.* **58** 2018 (in Chinese)

[18] Liu X C, Chen Z Z, Shi E W, Yan C F, Huang W, Song L X, Zhou K J, Cui M Q, He B and Wei S Q 2009 *Acta Phys. Sin.* **58** 0498 (in Chinese)

[19] Peng X D, Zhu T, Wang F W, Huang W G and Cheng Z H 2009 *Chin. Phys.* B **18** 2576

[20] Liu X C, Zhang H W, Zhang T, Chen B Y, Chen Z Z, Song L X and Shi E W 2008 *Chin. Phys.* B **17** 1371

[21] Schmidt-Mende L and MacManus-Driscoll J L 2007 *Mater. Today* **10** 40

[22] Lu Z L, Hsu H S, Tzeng Y H and Huang J C A 2009 *Appl. Phys. Lett.* **94** 152507

[23] Fons P, Iwata K, Yamada A, Matsubara, Niki S, Nakahara K, Tanabe T and Takasu H 2000 *Appl. Phys. Lett.* **77** 1801

[24] Cao Q, Deng J X, Liu G L, Chen Y X, Yan S S and Mei L M 2007 *Chin. Phys. Lett.* **24** 2951

[25] Pan F, Song C, Liu X J, Yang Y C and Zeng F 2008 *Mater. Sci. Eng.* R **62** 1

[26] Heald S M, Kaspar T, Droubay T, Shutthanandan V and Chambers S 2009 *Phys. Rev.* B **79** 075202

[27] Yin S, Xu M X, Yang L, Liu J F, Rösner H, Hahn H, Gleiter H, Schild D, Doyle S, Liu T and Hu T D 2006 *Phys. Rev.* B **73** 224408

[28] MacManus-Driscoll J L, Khare N, Liu Y L and Vickers M E 2007 *Adv. Mater.* **19** 2925

[29] Khare N, Kappers M J, Wei M, Blamire M G and MacManus-Driscoll J L 2006 *Adv. Mater.* **18** 1449

[30] Kittilstved K R, Schwartz D A, Tuan A C, Heald S M, Chambers S A and Gamelin D R 2006 *Phys. Rev. Lett.* **97** 037203

[31] Potashnik S J, Ku K C, Mahendiran R, Chun S H, Wang R F, Samarth N and Schiffer P 2002 *Phys. Rev.* B **66** 12408